



Co-Doping Effect of Mn and Y on Charge and Mass Transport Properties of BaTiO₃

CHUNG-EUN LEE,¹ SUN-HO KANG,^{1,*} DONG-SOOK SINN² & HAN-ILL YOO¹

¹*School of Materials Science and Engineering, Seoul National University, Seoul, 151-742, Korea*

²*Samsung Electro-Mechanics Co., Ltd., Suwon, Kyunggi-Do, 442-743, Korea*

Submitted March 3, 2003; Revised December 1, 2003; Accepted December 4, 2003

Abstract. BaTiO₃-based multilayer-ceramic capacitors (MLCC) using base metal (Ni) electrodes normally contains Mn and Y each approximately on the order of 0.5 mol%. It is only empirically known that the co-doping of Y and Mn facilitates sintering with the base-metal electrodes as well as improves the device performance and life time. In order to understand the effect of the co-doping, we have measured the electrical conductivity and chemical diffusivity on polycrystalline BaTiO₃ that is co-doped with Y and Mn each by 0.5 mol% against oxygen partial pressure at elevated temperatures. It is found that while the *n*-type conductivity in reducing atmospheres (e.g., $P_{O_2} < 10^{-6}$ atm at 1000°C) remains similar to that of undoped or acceptor-doped BaTiO₃, its *p*-type conductivity in oxidizing atmospheres (e.g., $P_{O_2} > 10^{-6}$ at 1000°C) is remarkably suppressed compared to the latter. The chemical diffusivity is also similar to that of the latter in magnitude (e.g., 10^{-2} – 10^{-5} cm²/s at 1000°C), but its trend of variation with oxygen partial pressure is rather opposite. These variations of the conductivity and chemical diffusivity are mainly attributed to Mn ions changing their valence from +2 to +3 to +4 with increasing oxygen partial pressure. It is explained from a defect-chemical view why the codoping of fixed-valent donor (Y) and variable-valent acceptor (Mn) has been practiced in MLCC processing.

Keywords: MLCC, BaTiO₃, acceptor-donor codoping, defect structure, chemical diffusivity

1. Introduction

Multilayer-ceramic capacitors (MLCC) consist of multi-layers of BaTiO₃-based dielectric with base metal (Ni) electrodes inserted in between. The as-formed MLCC should be sintered in a reducing atmosphere to keep the metal electrodes from oxidation. Once reduced, BaTiO₃, if pure, would become rich with oxygen vacancies and free electrons, and the latter lead to poor insulation resistance of the capacitors. A normal practice in processing MLCC is, thus, to add acceptor impurities so that they can trap reduction-induced electrons. Such acceptor impurities, however, enhances oxygen vacancy concentration, despite the post-sintering re-oxidation process, on the same level as the doped impurities (i.e., $[A_C^-] \approx 2[V_O^{\bullet\bullet}]$). Migra-

tion of these vacancies in electric fields at the service temperature eventually deteriorates the reliability and life time of the MLCC [1]. Design of MLCC compositions as well as processing routes, which can assure both the device performance and longevity, thus, appears to be in dilemma. It is recently reported that the life stability or reliability of MLCC may be improved by doping acceptor and donor impurities together [2]. In reality, a Y5V-type¹ Ni-MLCC composition which is known to have an excellent life time and stability contains MnO₂ and Y₂O₃ on the order of 0.5 mol% (relative to 100 Ba_{0.95}Ca_{0.05}Ti_{0.83}Zr_{0.17}O₃ for example) in addition to a similar amount of sintering aid. Nevertheless, design of MLCC compositions still remains an alchemy to some extent.

The present paper is concerned with the codoping effect of acceptor Mn and donor Y on charge and mass transport properties and hence, the defect structure of BaTiO₃ in comparison with undoped, only Mn-doped

*Current address: Chemical Technology Division, Argonne National Lab., U.S.A.

and only Y-doped ones. We consequently expect to understand why the codoping is profitably practiced in MLCC processing.

2. Experimental

Starting powders, BaTiO₃ (Aldrich, 99.995%), TiO₂ (Aldrich, 99.99%), MnO₂ (High Purity Chem., 99.99%) and Y₂O₃ (Aldrich, 99.99%) were intimately mixed in an ethanol media with zirconia balls into 4 different nominal compositions BaTiO₃·0.01TiO₂·xMnO₂·yYO_{1.5} with (i) $x = 0.000$, $y = 0.000$ (undoped); (ii) $x = 0.005$, $y = 0.000$ (acceptor-doped); (iii) $x = 0.000$, $y = 0.005$ (donor-doped); (iv) $x = 0.005$, $y = 0.005$ (codoped). These are henceforth designated as (i) “undoped,” (ii) “0.5Mn,” (iii) “0.5Y,” and (iv) “codoped,” respectively. The dried powders were calcined at 950°C in air for 10 h and subsequently reground in a pestle and mortar. The reground powders were molded into discs of ca. 25 mm dia., under a uniaxial pressure of 25 MPa and then pressed cold-isostatically under 150MPa for 5 min. Sintering was followed at 1350°C in air for 5 h. The as-sintered samples were found to be x-ray-wise phase-pure and ca. 90% dense with an average grain size of $15 \pm 6 \mu\text{m}$ (codoped).

The conductivity specimens were cut from the sintered disks into parallelepipeds measuring $1.6 \text{ mm} \times 1.6 \text{ mm} \times 15 \text{ mm}$. Equilibrium conductivity was measured as a function of oxygen partial pressure at elevated temperatures. The conductivity was subsequently evaluated from the as-measured conductance simply by taking into account the apparent geometric factor of the specimen without correcting against ca. 10% porosity of the specimen. Chemical diffusivity was measured by a d.c. conductivity relaxation technique upon an abrupt change of oxygen partial pressures in the surrounding. A change in oxygen partial pressure was controlled to be $\Delta \log(P_{\text{O}_2}/\text{atm}) \leq 1$. Ambient oxygen partial pressure was controlled in the range of 10^{-19} to 1 atm with N₂/O₂, N₂/CO₂ or CO₂/CO gas mixtures and monitored in situ by a zirconia-based oxygen sensor. For experimental details, the reader is referred to Ref. [3].

3. Results and Discussions

3.1. Equilibrium Conductivities

The equilibrium conductivities of the four different specimens (i) undoped, (ii) 0.5Mn, (iii) 0.5Y, and (iv)

codoped vary with oxygen partial pressure as shown in Figs. 1(a) and (b) at 1000°C and 1200°C respectively. Isothermal variation of conductivity is conventionally described as $\sigma \propto P_{\text{O}_2}^m$, where the oxygen exponent “ m ” is related to the majority type of disorder over a P_{O_2} region [4]. As is seen in Fig 1, the conductivity of the undoped specimen varies with $m \approx 1/4, -1/4, -1/6$ in sequence as P_{O_2} decreases from

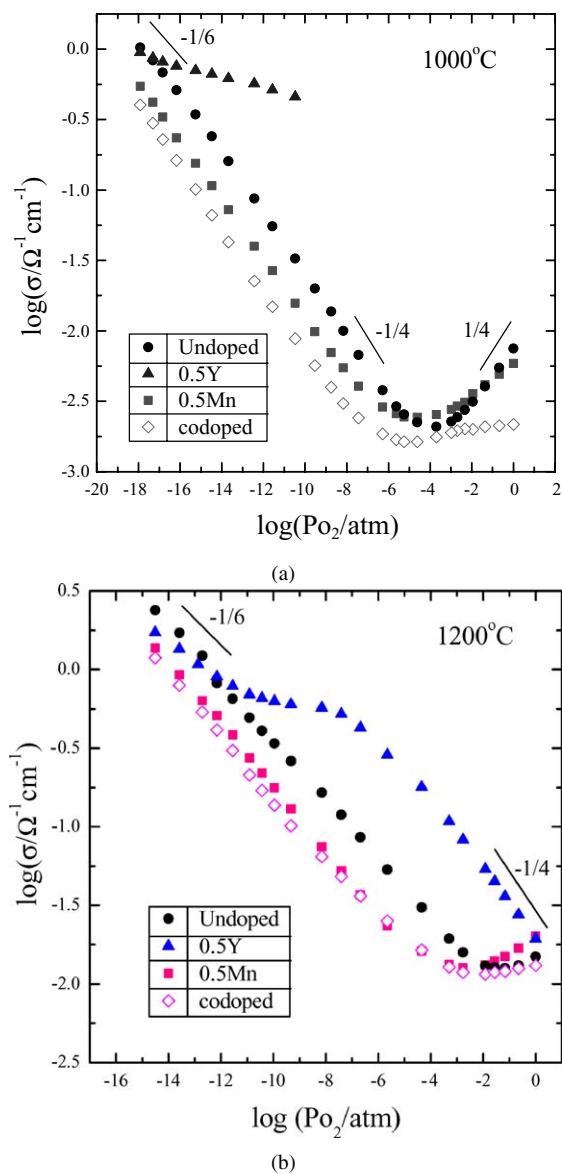


Fig. 1. Conductivity isotherms of undoped, 0.5 mol% Mn-doped, 0.5 mol% Y-doped, and 0.5 mol% Mn + 0.5 mol% Y codoped BaTiO₃, respectively, at 1000°C (a) and 1200°C (b).

1 atm. It has been repeatedly observed by different authors on undoped or (fixed-valent) acceptor-doped BaTiO₃[5]. The conductivity variation of the donor-doped specimen, 0.5Y is also in good agreement with the literatures [6, 7]: m takes the values, $-1/4; 0; -1/6$ in sequence with decreasing P_{O_2} from 1 atm. [The equilibration kinetics, however, was impractically sluggish in the oxygen activity range of $-10 < \log a_{O_2} < 1$ at 1000°C in particular and hence, data were missing there, see Fig. 1(a).] The effect of fixed-valent donor Y is quite conspicuous in comparison with the undoped. These variations of the undoped and donor-doped BaTiO₃ are rather well understood defect-chemically [5, 8].

The isotherm for the Mn-doped specimen, 0.5Mn may be described with a sequence of $m \approx +1/6; -1/6; -1/4; -1/6$ with decreasing P_{O_2} again in good agreement with literature [4]. This sequential variation of m was attributed to the change of valence of multi-valent Mn from +4 to +3 to +2 with decreasing oxygen partial pressure [4, 9], and the latter valence changes have recently been confirmed spectroscopically [9, 10].

Now, the conductivity variation of the codoped BaTiO₃ is somewhat peculiar. It is similar to that of the Mn-doped case in the n -type branch ($m < 0$), but in the p -type branch ($m > 0$), the conductivity appears to be suppressed compared to the undoped and Mn-doped cases. The suppression is more clearly seen in Fig. 2. One can see that as P_{O_2} increases in the p -type branch, the conductivity exponent even approaches $m \approx 0$.

This peculiar behavior of the codoped BaTiO₃ may be understood in terms of the change of the valence or acceptor effectiveness of the Mn ions with P_{O_2} in association with the fixed-valent donor Y_{Ba}^* . Defect structure of the codoped system may be described by taking into account the ionization equilibria of Mn as

$$O_O^\times = V_O^{\bullet\bullet} + 2e' + \frac{1}{2}O_2; \quad K_{Re} = [V_O^{\bullet\bullet}]n^2 P_{O_2}^{1/2} \quad (1)$$

$$0 = e' + h^*; \quad K_i = np \quad (2)$$

$$Mn_{Ti}^\times = Mn_{Ti}' + h^*; \quad K_1 = \frac{[Mn_{Ti}']p}{[Mn_{Ti}^\times]} \quad (3)$$

$$Mn_{Ti}' = Mn_{Ti}'' + h^*; \quad K_2 = \frac{[Mn_{Ti}']p}{[Mn_{Ti}']} \quad (4)$$

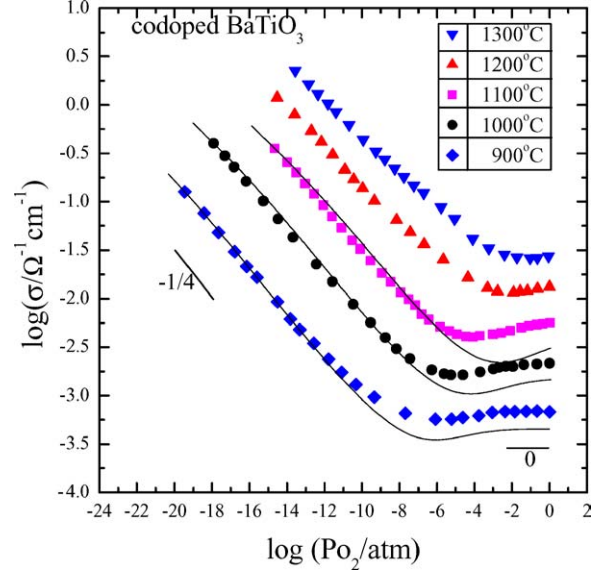


Fig. 2. Conductivity isotherms of 0.5 mol% Mn + 0.5 mol% Y codoped BaTiO₃ at different temperatures. Note the flattening trend in the p -type regime of oxygen partial pressure.

along with the mass conservation constraints for a codoped system

$$[Mn]_t = [Mn_{Ti}'] + [Mn_{Ti}'] + [Mn_{Ti}^\times] \quad (5a)$$

$$[Y]_t = [Y_{Ba}^*] \quad (5b)$$

and with the charge neutrality constraint,

$$n + [Mn_{Ti}'] + 2[Mn_{Ti}'] = p + [Y_{Ba}^*] + 2[V_O^{\bullet\bullet}] \quad (6)$$

Here, $[]$ denote the concentration of the defect therein, $n \equiv [e']$, $p \equiv [h^*]$, $[Mn]_t$ and $[Y]_t$ the total amount of Mn and Y doped, respectively, (for the present co-doped case, $[Mn]_t = [Y]_t$) and K_j the mass action law constant of the associated reaction j ($= Re, i, 1, 2$). One may define the effective acceptor concentration, $[A'_{eff}]$, as

$$[A'_{eff}] \equiv [Mn_{Ti}'] + 2[Mn_{Ti}'] - [Y_{Ba}^*] \quad (7)$$

By using the numerical values for K_j that are available in literatures [4, 9, 18], one calculates the

concentrations of defects e.g., at 1000°C for the Mn-doped (0.5 Mn) and the codoped ($[Mn]_t = [Y]_t$) to obtain the results as in Figs. 3(a) and (b), respectively. As is seen, the two majority types of disorder, $n \approx 2[V_O^{\bullet\bullet}]$ and $2[V_O^{\bullet\bullet}] \approx [A'_{eff}]$ dominate the overall P_{O_2} range examined. It is like undoped or fixed-valent acceptor-

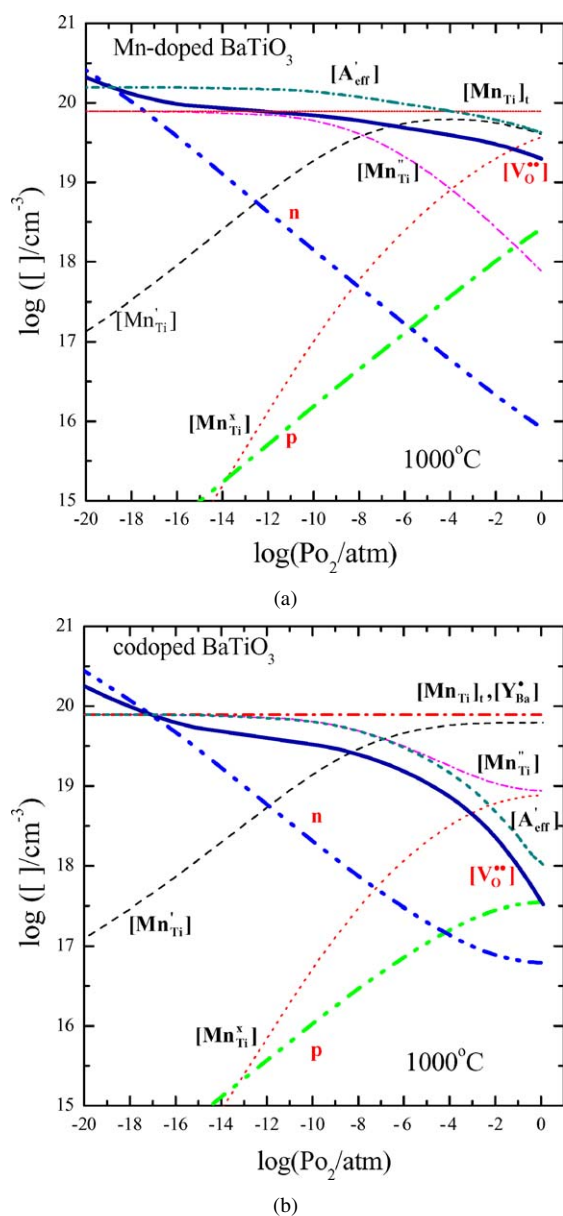


Fig. 3. Calculated defect concentrations [] vs. oxygen partial pressure at 1000°C for 0.5 mol% Mn-doped (a) and 0.5 mol% Mn + 0.5 mol% Y codoped BaTiO₃ (b). Note the effect of donors (Y) on the effective acceptor concentration $[A'_{eff}]$ and hence, $[V_O^{\bullet\bullet}]$.

doped cases [5], but while it remains fixed in the former because the acceptors are fixed-valent, $[A'_{eff}]$ is decreasing with increasing oxygen partial pressure for the Mn-doped cases due to the change of valence of Mn or Eqs. (3) and (4). Upon comparison, one can recognize that by codoping of the same amount of fixed-valent donors $[Y_{Ba}^i]$, reduction of $[A'_{eff}]$ and hence, $[V_O^{\bullet\bullet}]$ is rendered more effective as P_{O_2} increases. The faster reduction of $[V_O^{\bullet\bullet}]$ with increasing P_{O_2} leads to the more effective suppression of p , see Eqs. (1) and (2).

One can now understand why the conductivity of the codoped specimen should be as in Fig. 2 from the variations of n and p in Fig. 3(b). The solid curves in Fig. 2 are the calculated conductivities at 900°, 1000° and 1100°C [from n and p in Fig. 3(b)] by estimating the mobility of electrons $[\mu_n (= \sigma_n/en) = 0.022, 0.022$ and $0.018 \text{ cm}^2/V \cdot \text{s}$ at 900°, 1000° and 1100°C, respectively] from the essentially n -type conductivity (σ_n) in Fig. 2 and n in Fig. 3 and by assuming $\mu_p \approx \mu_n$ as the mobility ratio of electrons to holes is not much different from 1 at elevated temperatures [11, 12]. The calculated (solid lines) satisfactorily depict the trend of conductivity and the discrepancy of the values in the p -type branch may be attributed to the uncertainty of the K_j -values used for the calculation of n and p in Fig. 3 and/or the assumption with respect to the hole mobility.

It is clearly seen that by codoping of the variable-valent acceptor Mn and fixed-valent donor Y in proper proportion, one can suppress more effectively the concentration of oxygen vacancies at oxidizing atmosphere and hence, this fact may help design MLCC compositions for better performance and longevity.

3.2. Chemical Diffusivities

Degree of equilibration in terms of electrical conductivity $[(\bar{\sigma}(t) - \sigma(0))/(\sigma(\infty) - \sigma(0))]$, see Eq. (9) below] upon a sudden change of oxygen partial pressure are typically as shown in Fig. 4. The Mn-doped (0.5Mn) and codoped are very fast in re-equilibration (fully equilibrated within less than 1 hr), but the Y-doped (0.5Y) is extremely sluggish (not equilibrated yet even after 1 day). It is well known that oxygen nonstoichiometry reequilibration kinetics is very fast for undoped or acceptor doped BaTiO₃[11, 13–15, 18], but very sluggish for donor doped BaTiO₃[15–17]. One may, thus, generalize that as long as $[A'_{eff}] > 0$, the reequilibration kinetics is much faster than otherwise.

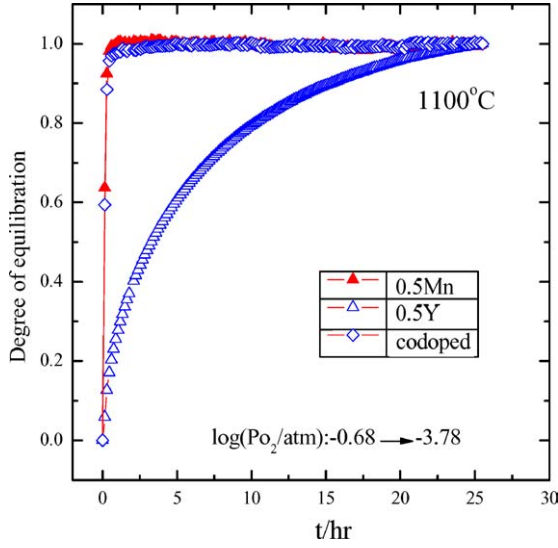


Fig. 4. Degree of oxygen re-equilibration vs. time upon a change of oxygen partial pressure from $\log(P_{O_2}/\text{atm}) = -0.68$ to -3.78 for 0.5 mol% Mn-doped, 0.5 mol% Y-doped, and 0.5 mol% Mn + 0.5 mol% Y codoped BaTiO_3 , respectively, at 1100°C . Note that the donor-doped is much more sluggish.

Quantitative analyses of the conductivity relaxations for the Mn-doped and codoped are not so simple as for the fixed-valent acceptor-doped case, e.g. Al-doped BaTiO_3 [18] where the electronic carrier concentration is a direct measure of oxygen vacancy concentration or nonstoichiometry only [i.e., $\partial[A'_{\text{eff}}]/\partial t = 0$ in Eq. (8) below]. In the present cases with variable-valent acceptor Mn, however, due to Eqs. (6) and (7),

$$\frac{\partial}{\partial t}(n - p) = 2\frac{\partial}{\partial t}[V_{\text{O}}^{\bullet\bullet}] - \frac{\partial}{\partial t}[A'_{\text{eff}}] \quad (8)$$

Detailed solution to the problem is out of the scope of the present paper. In order only to evaluate a measure of the reequilibration kinetics of the codoped case that is corresponding to the chemical diffusivity of oxygen for undoped or fixed-valent acceptor-doped BaTiO_3 [11, 18], one may simply assume that the overall kinetics is governed by the chemical diffusion of oxygen and surface reaction to use the solution for either $n \gg p$ or $n \ll p$ for the geometry of the present specimens [3]:

$$\frac{\bar{\sigma}(t) - \sigma(0)}{\sigma(\infty) - \sigma(0)} = 1 - \left(\sum_{n=0}^{\infty} \frac{2L^2}{\beta_n^2(\beta_n^2 + L^2 + L)} \exp\left[-\frac{\beta_n^2 \tilde{D}t}{a^2}\right] \right)^2 \quad (9a)$$

with β such that

$$\beta \tan \beta = L; \quad L = \frac{ak}{\tilde{D}} \quad (9b)$$

Here, $\bar{\sigma}(t)$, $\sigma(0)$ and $\sigma(\infty)$ stand for the (spatial) average conductivity at time t , $t = 0$ and $t = \infty$, respectively, “ $2a$ ” a dimension of the square cross section of the parallelepipeds specimens, k the surface reaction rate constant, and \tilde{D} the apparent chemical diffusivity.

The conductivity relaxation data are fitted to Eq. (9) to evaluate the apparent diffusivity. Typical results are as shown in Fig. 5. As is seen, Eq. (9) describes quite well the relaxation kinetics and hence, the assumption with respect to Eq. (9) may be justified *a posteriori*.

The apparent chemical diffusivity as evaluated on the codoped specimen is shown in Fig. 6 in comparison with that of fixed-valent acceptor (Al)-doped one [18]. It is seen that the chemical diffusivity is comparable to that of the acceptor(Al)-doped single crystal BaTiO_3 , but its variation against P_{O_2} is quite distinct from the latter. This variation may also be understood in terms of the valence change of Mn. The apparent diffusivity for the present case is believed to be essentially the chemical diffusivity of oxygen. When oxide ions and electrons are mobile in BaTiO_3 , the chemical

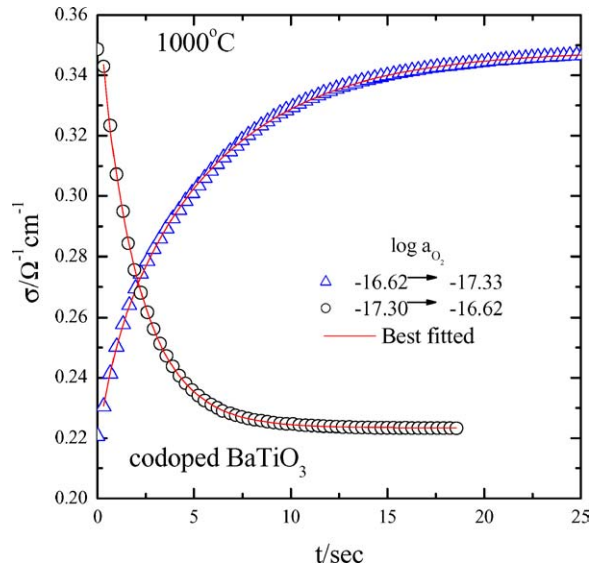


Fig. 5. Relaxation of the conductivity as measured upon reduction and oxidation for 0.5 mol% Mn + 0.5 mol% Y codoped BaTiO_3 at 1000°C . The solid lines are the best fitted curves to Eq. (9) in the text.

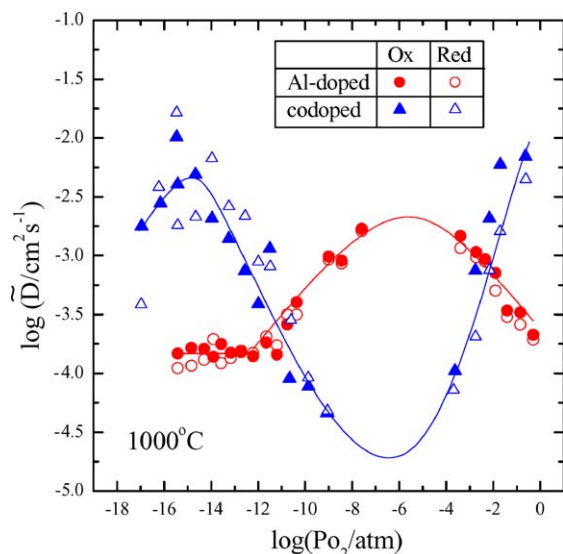


Fig. 6. Apparent chemical diffusivity of 0.5 mol% Mn + 0.5 mol% Y codoped BaTiO₃ vs. oxygen partial pressure in comparison with the chemical diffusivity of oxygen of 1.8 mol% Al-doped, single crystal BaTiO₃ from Ref. [18]. The solid line for the Al-doped is the calculated one; that for the codoped for visual guidance only.

diffusivity of the chemical component oxygen is given in accordance with Wagner as [11, 19]

$$\tilde{D} \cong -\frac{D_V t_{el}}{2} \left[\frac{\partial \ln[V_O^{\bullet\bullet}]}{\partial \ln P_{O_2}} \right]^{-1} \quad (10)$$

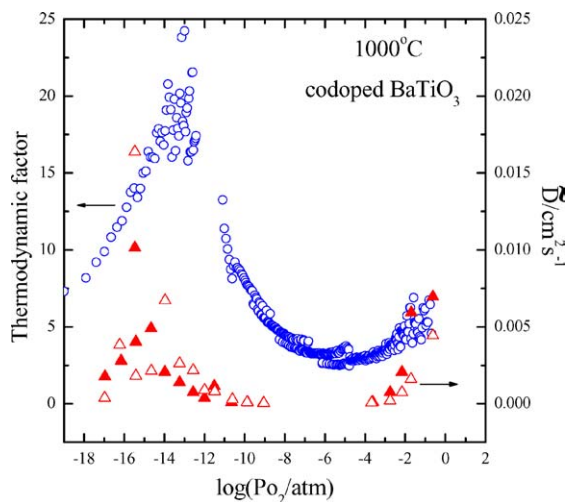


Fig. 7. Apparent chemical diffusivity and the thermodynamic factor of 0.5 mol% Mn + 0.5 mol% Y codoped BaTiO₃ at 1000°C. It is noted that the thermodynamic factor delineates the variation of the chemical diffusivity.

where D_V is the diffusivity of oxygen vacancies and t_{el} the electronic transference number. For the present case, $t_{el} \approx 1$. The thermodynamic factor within the brackets is nothing but the inverse of the slope of the curve for $[V_O^{\bullet\bullet}]$ in Fig. 3(b), that is shown in Fig. 7 in comparison with the apparent diffusivity as measured. One can recognize that the variation of the latter is attributed to that of the thermodynamic factor as has been the case for undoped or acceptor-doped BaTiO₃ [11, 18].

4. Conclusion

It is confirmed that codoping of Mn and Y in proper proportions can suppress more effectively the concentrations of oxygen vacancies and holes in the p -type regime of BaTiO₃ (i.e., in post-sintering atmospheres of MLCC), thus improving the performance reliability and life time of MLCC. It is attributed to variable-valent acceptor Mn taking a valence from 2 to 3 to 4 with increasing oxygen activity, thus rendering itself less and less effective as acceptors. Oxygen re-equilibration kinetics of the codoped BaTiO₃ is as fast as for undoped or acceptor-doped BaTiO₃. The variation of the apparent diffusivity as a measure of the re-equilibration kinetics with oxygen partial pressure is also delineated by the variation of the valence change of Mn via the thermodynamic factor. Codoping of variable-valent acceptors and fixed-valent donors in proper proportions may, thus, be profitably employed to design MLCC compositions with better performance and longevity.

Acknowledgments

This work was supported by the Center for Advanced Materials Processing under “21C Frontier Program” of the Ministry of Science and Technology, Korea.

Note

1. An EIA (Electronic Industries Association) specification.

References

1. T. Baiatu, R. Waser, and K.-H. Hardtl, *J. Am. Ceram. Soc.*, **73**, 1663 (1990).

2. S. Sato, Y. Nakano, A. Sato, and T. Nomura, *J. Eur. Ceram. Soc.*, **19**, 1061 (1999).
3. C.-R. Song and H.-I. Yoo, *Solid State Ionics*, **120**, 141 (1999).
4. J.-Y. Kim, C.-R. Song, and H.-I. Yoo, *J. Electroceram.*, **1**, 27 (1997).
5. H.-I. Yoo, C.-R. Song, and D.-K. Lee, *J. Electroceram.*, **8**, 5 (2002).
6. J. Daniels and K.H. Härdtl, *Philips Res. Rep.*, **31**, 489 (1976).
7. N.H. Chan and D.M. Smyth, *J. Am. Ceram. Soc.*, **67**, 285 (1984).
8. D.M. Smyth, *The Defect Chemistry of Metal Oxides* (Oxford University Press, Oxford, 2000), Chap. 14
9. D.-K. Lee, H.-I. Yoo, and K.D. Becker, *Solid State Ionics*, **154**, 189 (2002).
10. J. Klages, Diploma Thesis, Institute of Physical and Theoretical Chemistry, Technical University of Braunschweig, Germany (2003).
11. C.-R. Song and H.-I. Yoo, *Phys. Rev. B*, **61**, 3975 (2000).
12. N.H. Chan, R.K. Sharma, and D.M. Smyth, *J. Am. Ceram. Soc.*, **64**, 556 (1981).
13. A. Müller and K.-H. Härdtl, *Appl. Phys. A*, **49**, 75 (1989).
14. J. Maier, G. Schwitzgebel, and H.-J. Hagemann, *J. Solid State Chem.*, **58**, 1 (1985).
15. R. Wernicke, *Philips Res. Rep.*, **31**, 526 (1976).
16. J. Nowotny and M. Rekas, *Ceram. Int.*, **20**, 265 (1994).
17. H.-I. Yoo and C.-E. Lee, *Phys. Rev. B*, (submitted).
18. C.-R. Song and H.-I. Yoo, *J. Am. Ceram. Soc.*, **83**, 773 (2000).
19. C. Wagner, *Z. Phys. Chem. Abt. B*, **21**, 25 (1933).